Lasing of nanoemitters with nanorings having Drude dispersion

Nanoemisores láser con nanoanillos que tienen dispersión Drude

Gennadiy Burlak[1,*] and Gustavo Medina-Ángel[1]

[1]Centro de Investigación en Ingeniería y Ciencias Aplicadas, (CIICAp). Universidad Autónoma del Estado de Morelos
Av. Universidad No. 1001, Col. Chamilpa, 62209, Cuernavaca, Morelos, México
[*]gburlak@uaem.mx

KEYWORDS:

Nanoemitters, nanorings, laser emission, plasmon-polariton

ABSTRACT

TWe systematically study the dynamics and laser emission of randomly distributed nanoemitters (NEs) integrated into two-dimensional (2D) array of metal nanorings (NR) enhanced by the plasmon-polariton (PP) excitations. It is shown that the transition time to the laser generation regime (instability) of NE optical fields significantly depends on the plasma frequency ωp of the NR. The PP fields is excited macroscopically in the whole system if ωp of NR exceeds a certain critical transition value $\omega p > \omega c$. The latter leads to a strong coupling of the NE emission with the PP fields and a critical increase of the total current in the NR array. We found the analytical dependence of the critical current amplitude $I = I(\omega p/\omega c)$ as function of NR plasma frequency, which is in a good agreement with the numerical simulations.

PALABRAS CLAVE:

Nanoemisores, nanoanillos, emision laser, plasmon-polariton

RESUMEN

Estudiamos sistemáticamente la dinámica y la emisión láser de nanoemisores (NE) distribuidos aleatoriamente integrados en una matriz bidimensional (2D) de nanoanillos metálicos (NR) mejorados por las excitaciones de plasmón-polaritón (PP). Se muestra que el tiempo de transición al régimen de generación de láser (inestabilidad) de los campos ópticos NE depende significativamente de la frecuencia del plasma ωp del NR. Los campos PP se excitan macroscópicamente en todo el sistema si ωp de NR excede un cierto valor de transición crítico $\omega p > \omega c$. Esto último conduce a un fuerte acoplamiento de la emisión de NE con los campos de PP y a un aumento crítico de la corriente total en el conjunto de NR. Encontramos la dependencia analítica de la amplitud de la corriente crítica $I = I(\omega p/\omega c)$ en función de la frecuencia del plasma NR, lo que concuerda bien con las simulaciones numéricas.

• **Recibido: 30 de agosto de 2023** • **Aceptado: 28 de octubre de 2023** • **Publicado en línea: 1 de octubre de 2024**

1. INTRODUCTION

Nowadays, investigations of aligned carbon nanostructures have stimulated various spectroscopic studies on a spatial scale of several nanometers [1,2,3,4,5,6,7,8,9,10] [11,12]. Considerable interest is devoted to study linear and nonlinear plasmonic properties of nanohybrids and nanocomposites made of metallic nanoparticles and quantum emitters (QEs) [13,14,15,16,17]. The inclusion of dispersed

DOI: 10.30973/progmat/2024.16.3/1

single-walled carbon nanotubes (SWCNTs) in the working space of QEs or nanoemitters (NEs) considerably changes the properties of the electromagnetic field, whose structure depends significantly on the plasma frequency ωp of SWCNTs. In such a hybrid system, it becomes possible to control the properties of local optical fields that allows creating of miniature low threshold coherent sources with tunable polarization [18, 6]. For the low frequency spectrum, such a medium behaves like a system of dielectric cylinders with the well-known properties of Bloch waves [19]. But for high frequencies, in the system already dominate the dynamic properties of electromagnetic waves in plasma cylinders, where the surface plasmons can propagate. In the intermediate frequency region, the fields acquire a complex structure in the area of cut-off of plasmonic wave modes. The spectral properties of such modes in SWCNTs in the ideal case of lossless and infinite SWCNTs have been well-studied in quantum and quasiclassical approximations [20,21,22,23].

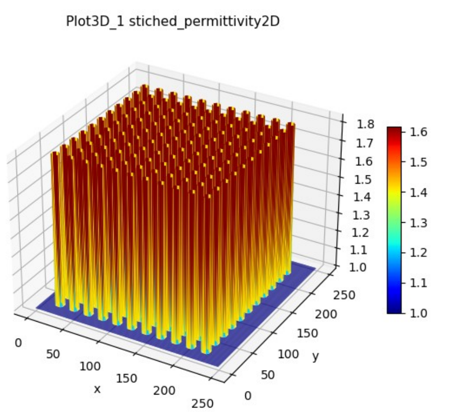

Figure 1. The array of nanorings (NR) with external radius R dielectric permittivity ε∞ = 1.8 and width of the well w, periodically placed on a dielectric substrate.

However, in real case of finite and lossy SWCNTs, new factors become to play an important role. The plasmonic fields of dispersing nanotubes perturb the energy levels of the NE and, thus, the PPs in SWCNTs appear to be related to the inner degrees of freedom of the NEs. An important property of NEs is the nonlinearity of the field and the possibility of the laser generation [24]. In such a hybrid system, the lasing threshold in the NE depends on the spatial structure of randomly distributed NEs. It is found that all mentioned factors can establish of a resonant change in the field structure associated with the PP generation in SWCNTs.

2. GEOMETRY

We consider the (metal) nanorings (NR) having external radius R and width of the well w periodicaly placed in 2D dielectric substrate, see Fig.1. (Here the colorbar indicates the static dielectric permitttivity of ND).

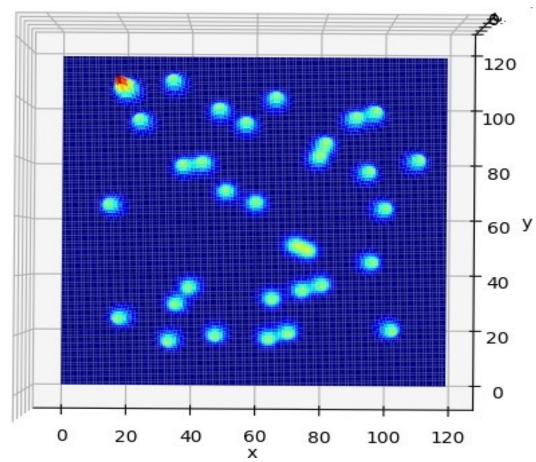

Figure 2. Initial distribution of 33 NE in the 2D nanorings array (see Fig. 1).

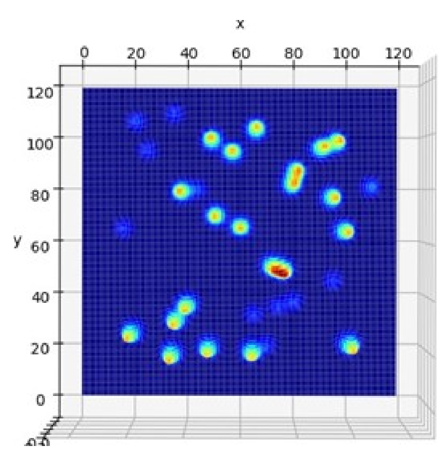

Figure 3. Optical field PP structure in the 2D NR array (see Fig. 1) with NE at small time t = 19 before the lasing of NE begins.

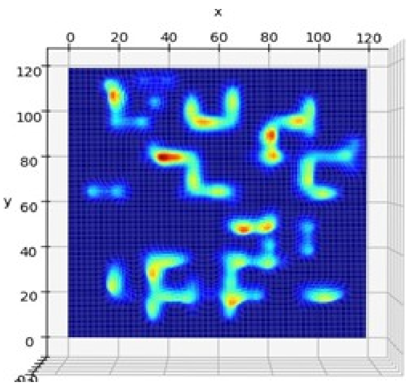

Figure 4. Optical PP field structure in 2D NR array (see Fig. 1) with lasing of NE (t = 39) and the field interconnections between NR.

3. BASIC EQUATIONS

In considered hybrid system the Maxwell equations read:

$$\nabla\times\boldsymbol{E} \;=\; -\mu_0\frac{\partial\boldsymbol{H}}{\partial t},\;\; \nabla\times\boldsymbol{H}=\varepsilon_0\frac{\partial\boldsymbol{E}}{\partial t}+\boldsymbol{J_e}+\sigma_e\boldsymbol{E}+\sum_k \boldsymbol{I_k}\boldsymbol{P_k}(\boldsymbol{R_k},t)\,\delta_{rRk}, \quad (1)$$

where $\mathbf{J}_e$ is the electrical current in NR, t is the time, $\mathbf{E}$ and $\mathbf{H}$ are the electric and magnetic fields respectively, which obeys the material equation [25].

$$\boldsymbol{J_e}+\gamma_e\boldsymbol{J_e}=b_e\boldsymbol{E}, \quad (2)$$

where γ_e is the collision frequency in NR, $b_e=\varepsilon_0\omega_p^2$, ω_p is the plasma frequency, σ_e is conductivity, and, ε_h is the dielectric constant of the host medium of NR. In Eq.(1) $\boldsymbol{I_k}=\frac{\partial\boldsymbol{P_k}}{\partial t}$ and $\mathbf{P_k}(\mathbf{R}_k,t)$ (k=1,N) is the polarization density produced by N NEs in positions $\mathbf{R}_k$. Following the single electron case, the equation for $\mathbf{P}_k$ in the vicinity of the emitters is [24].

$$\frac{\partial^2\boldsymbol{P}_k}{\partial t^2}+\Delta\omega_a\frac{\partial\boldsymbol{P}_k}{\partial t}+\omega_a^2\boldsymbol{P}_k=\frac{6\pi\epsilon_0 c^3}{\tau_{21}\omega_a^2}\left(N_{1,k}-N_{2,k}\right)\boldsymbol{E}_k. \quad (3)$$

To complete the model, we add the rate equations [24] for the occupation levels of emitters $N_{i,k}=N_i(\mathbf{R_k}, t)$ (following [17], we consider that the NEs are four-level quantum systems or quantum dots (QD)):

$$\frac{\partial N_{0,k}}{\partial t}=-A_r N_{0,k}+\frac{N_{1,k}}{\tau_{13}},\;\; \frac{\partial N_{3,k}}{\partial t}=A_r N_{0,k}-\frac{N_{3,k}}{\tau_{02}}, \quad (4)$$

$$\frac{\partial N_{1,k}}{\partial t}=\frac{N_{2,k}}{\tau_{32}}-M_k-\frac{N_{1,k}}{\tau_{13}},\;\; \frac{\partial N_{2,k}}{\partial t}=\frac{N_{1,k}}{\tau_{12}}+M_k-\frac{N_{2,k}}{\tau_{02}}, \quad (5)$$

$$M_k=\frac{(\boldsymbol{j}\cdot\boldsymbol{E})_k}{\hbar\omega_a},\;\; j_k=\frac{\partial\boldsymbol{P}_k}{\partial t}.$$

Here $\Delta\omega_a=\tau_{21}^{-1}+2T_{21}^{-1}$, where T_2 is the mean time between dephasing events, τ_{21} is the decay time from the second atomic level to the first one, ω_a is the frequency of radiation (see e.g. [24]), and A_r is a certain pumping rate, which is proportional to the pumping intensity in experiments. In our simulations we considered the gain medium with parameters close GaN powder, similar to Ref. [26]. The lasing frequency ω_a is $2\pi\times3\times10^{13}$ Hz, the lifetimes are τ_{32}=0.3 ps, τ_{10}=1.6 ps, τ_{21}=16.6 ps, and the dephasing time is T_2=0.0218 ps. The nonlinear quasi-classical system (1)-(5) cannot be solved analytically in general; therefore, below we use the numerical Finite Difference Time Domain (FDTD) simulations (in the output we impose the absorbing boundary conditions (ABC)) [25]. The later allowing us to obtain the exact solutions to system (1)-(5). In what follows we use the dimensionless time t renormalized as $t\to tc/l_0$, where $l_0=100\mu m$ is the typical spatial scale and c is the light velocity in the vacuum.

4. PLASMONS IN NANORING

In this Section we start to discuss the properties of a simplest plasmonic modes in a single cylindrical nanoperticle [20,21,22] as a lossless, infinitesimally thin cylindrical shell with radius R, where the valence electrons are considered as a free-electron gas distributed uniformly over the cylindrical surface, with the density per unit area n_0. It is used the cylindrical coordinates r=(ρ, φ, z) and considered an electromagnetic wave with frequency ω, propagating along the nanoring axis z. The homogeneous electron gas is perturbed by the electromagnetic wave and can be regarded as a charged fluid with the velocity field $v(r_S, t)$ and the perturbed density (per unit area) $n_1(r_S, t)$, where $r_S=(\varphi, z)$ are the coordinates of a point at the cylindrical surface of the nanoring. The electronic excitations on the cylindrical surface surface can be described by the following (linearized) continuity equation and the momentum-balance equation respectively [22].

$$\frac{\partial}{\partial t}n_1+n_0+\nabla_{\|}v_1=0, \quad \frac{\partial}{\partial t}v_1=\frac{-e}{m_e}\boldsymbol{E}_{\|}-\frac{\alpha}{n_0}\nabla_{\|}n_1+\frac{\beta}{n_0}\nabla_{\|}(\nabla_{\|}^2 n_1 \tag{6}$$

$$\frac{\partial}{\partial t}\rho_1+n_0+\nabla_{\|}j_1=0, \quad \frac{\partial}{\partial t}j_1=\frac{-e^2 n_0}{m_e}\boldsymbol{E}_{\|}-\frac{\alpha n_0}{n_0}\nabla_{\|}\rho_1+\frac{\beta n_0}{n_0}\nabla_{\|}(\nabla_{\|}^2\rho_1), \tag{7}$$

where E_I is the tangential component of the electromagnetic field, e is the element charge, and m_e is the electron mass, $\rho_1=en_1$, $j_1=en_0v_1$, and coefficients α, β describe single electron excitations in the 2D electron gas. In particular, $\alpha=v_F^2$ is the speed of propagation of the density disturbances in the electron gas with $v_F=(2\pi n_0 a_B^2)^{1/2}v_B$ being the Fermi velocity of the 2D electron gas and $\beta=(a_B v_B)^2/4$ describes single-electron excitations in the electron gas. Here a_B and v_B are the Bohr radius and the Bohr velocity, respectively.

In the follows we will use the simple Drude model, where the equation for electical current j_k in k-th nanoring reads

$$\frac{\partial_{jk}}{\partial t}+\gamma j_k=\epsilon_0\omega_p^2 E \tag{8}$$

were ω_p^2 is the plasma frequency , γ is the loss (phenomenological inverse relaxation time). The total electric current of the plasmons in all the nanorings in the system can be written as

$$J=\sum_{k=1}^{N} j_{1k}$$

where N is the number of nanorings. Due to the cylindrical symmetry of a NP we replace ρ_1, j_1 and the fields in the Maxwell's equations $\nabla\times\mathbf{E}=-\partial\mathbf{B}/\partial t$, $\nabla\times\mathbf{B}=c^{-2}\partial\mathbf{E}/\partial t$ by the Fourier forms

$$[E(r,\varphi,z,t),B(r,\varphi,z,t)]=\sum_{m=-\infty}^{m=+\infty}\int_{-\infty}^{\infty}dq[E(r,q),B(r,q)]\exp i(m\varphi+qz-\omega t),$$

where m is the integer azimuth quantum number, and q is the longitudinal wave vector. Substituting these expressions into boundary conditions, we obtain the dispersion relation between the frequency ω and the wave number k (TE modes) in the following dimensionless form:

$$D_{TE}(x,y)\equiv y^2-\alpha_1(x^2+\sigma y^2+m^2)-\beta_1(x^2+\sigma y^2+m^2)^2-x\,I'_m(x)\,K'_m(x)=0, \tag{9}$$

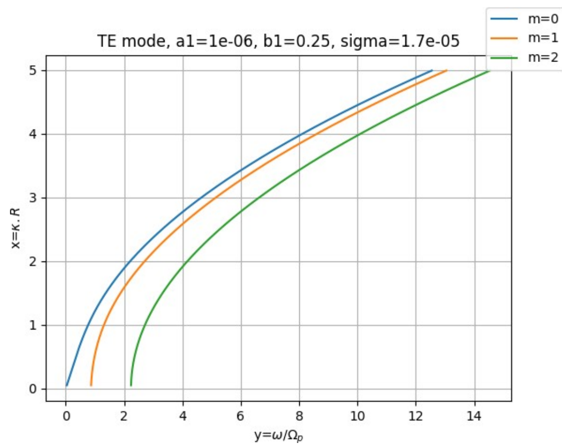

Figure 5. Dispersion dependence for TE waves for case of nonzero coefficients a1 and b1 in the dispersion Eq. (9).

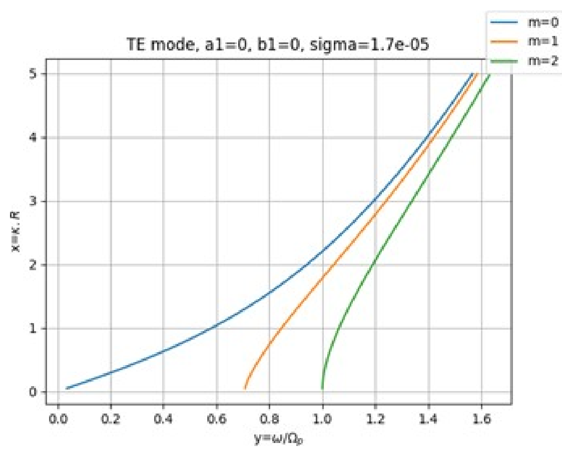

Figure 6. Dispersion dependence for TE waves for case of zero coefficients a1 and b1 in the dispersion Eq. (9).

$$D_{TE}(x,y)\equiv y^2-\alpha_1(x^2+\sigma y^2+m^2)-\beta_1(x^2+\sigma y^2+m^2)^2-x^{-2}(x^2+\sigma y^2+m^2)\,I_m(x)\,K_m(x)=0, \tag{10}$$

where $y=\omega/\Omega_p$, $x=\kappa R$, $\kappa^2=q^2-k^2$, $k=\omega/c$ is the wave number, c is the light speed, R is radius of nanoring. In Eq. (10) $\Omega_p=(e^2 n_0/\varepsilon_0 m_e R)^{1/2}$, $I'_m(x)$ and $K'_m(x)$ denote the derivatives of the modified Bessel functions with respect to argument [27], and ε_0 is the permittivity of free space, $\alpha_1=\alpha(\omega_p R)^2$, $\beta_1=(\Omega_p^2 R^4)$, and $\sigma=\Omega_p^2 R^2/c^2$.

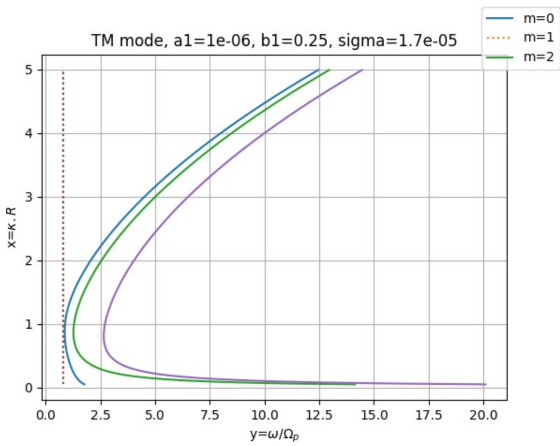

Figure 7. Dispersion dependence for TM waves for case of non zero coefficients a1 and b1 in the dispersion Eq. (10).

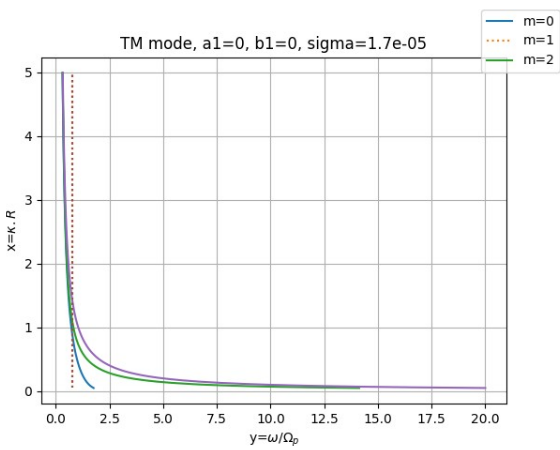

Figure 8. Dispersion dependence for TM waves for case of zero coefficients a1 and b1 in the dispersion Eq. (10).

The eigenvalues $\omega^2=[\omega_m(q)]^2$ obtained by solving (10) represent the plasmon dynamics in the infinitely long and lossless nanoring. Fig. 7 shows the solution of Eq. (10) for $x=\kappa R$ as function of $y=\omega/\Omega_p$ at different m. One can see that the dispersion curves κR for the nanoring increase with increasing the value ω of for all $m\geq 0$, and approach the plasmon frequency of the 2D electron gas $y^2=x/2$ [19]. Since the azimuth symmetric m=0 plasmon mode normally does not contribute to the high-frequency plasmons [28], we will consider the frequency range $\omega>\omega_c$, where ω_c is the cut-off frequency for the first azimuthal asymmetric m=1 mode of plasmon (at $y\approx 0.7$, see Fig 8) We evaluate ω_c for the charge density $n_0=2.15\times 10^{13} m^{-2}$ and R=2.4nm when Ω_p is about $2\pi\times 0.34$ THz that, as Fig. 8 shows, for m=1 corresponds to $\omega_c=2\pi\times 0.24$ THz.

In what follows, such a frequency ω_c can be mentioned as a critical value at that the asymmetric plasmons can be generated and coupled to the field of embedded NEs. However the study of plasmon dynamics in a simple model of lossless, infinite nanorings is too simplified. Numerical studies are needed to investigate the details of PPs in a periodic array of finite and dispersive NR, where the field interconnections and coupling the plasmon field to embedded NEs are possible.

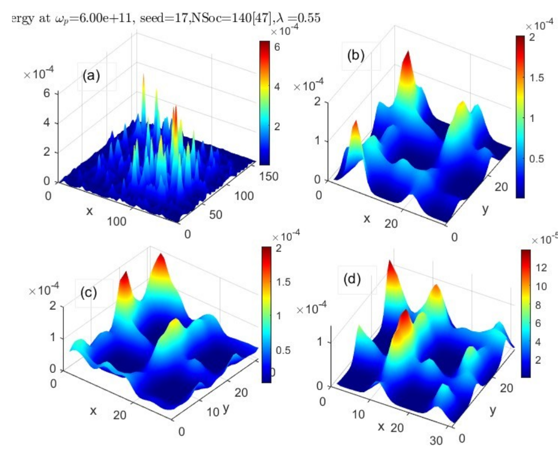

Figure 9. Spatial distribution of the average PP field energy (arbitrary units) at ωp=0.6THz and Ne=47 radiated NE: (a) the energy distribution in the complete NR array; (b) views the energy in the local rectangular [30, 30; 60, 60]; (c) [35, 35; 65, 65]; (d) [40, 40; 70, 70] respectively. It is seen that the energy is concentrated mainly in the gaps and the field practically does not penetrate inside NRs. For such value ωp=0.6THz the typical scale of the amplitude of PP field energy$\simeq 10^{-4}$.is negligible small with respect of cases with larger ωp>1.0THz, see figures below.

CONCLUSION

We have studied the dynamics and laser emission of randomly distributed nanoemitters (NEs) integrated into two-dimensional (2D) array of metal nanorings

(NR) enhanced by the plasmon-polariton (PP) excitations. It is shown that the transition time to the laser generation regime (instability) of NE optical fields significantly depends on the plasma frequency ωp of the NR. The PP fields is excited macroscopically in the whole system if ωp of NR exceeds a certain critical transition value $\omega p > \omega c$. The latter leads to a strong coupling of the NE emission with the PP fields and a critical increase of the total current in the NR array.

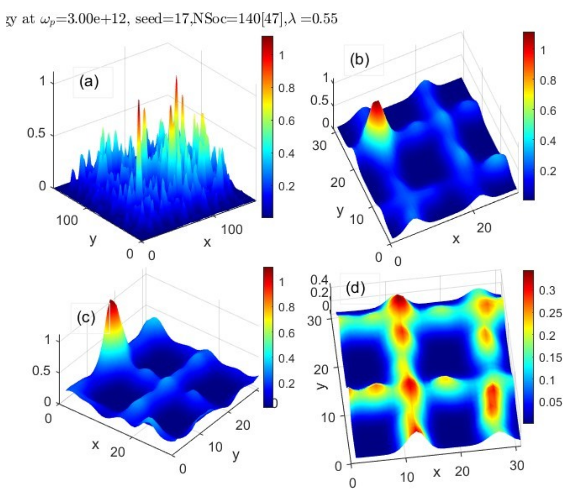

Figure 10. The same as in Fig. 9 but for ωp=6.0*THz*. Besides, we observe that for this ωp=6*THz* the typical scale of the field energy is ~ 1 that is at 4 orders larger with respect of the case ωp=0.6*THz* shown on Fig. 9.

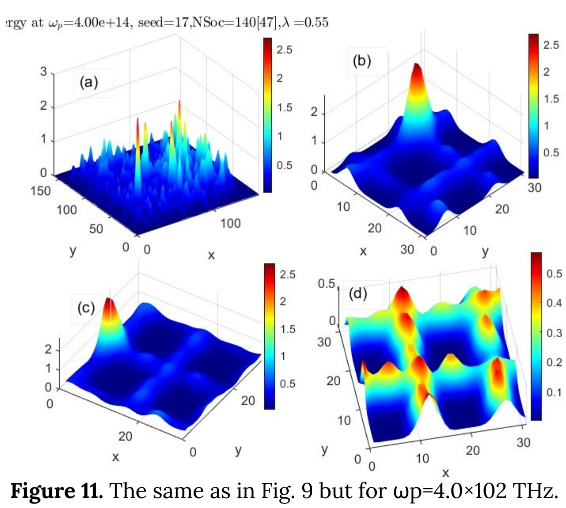

Figure 11. The same as in Fig. 9 but for ωp=4.0×102 THz.

Acknowledgments

This work was supported, in part, by CONACYT (México) through grants No. A1-S-9201 and No. A1-S-8793. G. M-A. acknowledges an fellowship provided by the CONACyT-México.

REFERENCES

[1] AlAloul M, Rasras M. Plasmon-enhanced graphene photodetector with CMOS-compatible titanium nitride. Journal of the Optical Society of America B. 2021, 38(2), 602-610. doi: 10.1364/JOSAB.416520.

[2] Eatemadi A, Karimkhanloo H, Daraee H, Kouh M, Zargham N, Akbarzadeh A, Joo SW. Carbon nanotubes: properties, synthesis, purification, and medical applications. Nanoscale research letters. 2014, 9, 1-13. doi: 10.1186/1556-276X-9-393.

[3] De Angelis F, Das G, Candeloro P, Patrini M, Galli M, Bek A, Lazzarino M, Maksymov I, Liberale C, Andreani LC, Di Fabrizio E. Nanoscale chemical mapping using three-dimensional adiabatic compression of surface plasmon polaritons. Nature Nanotech. 2010, 5(1), 67-72. doi: 10.1038/nnano.2009.348.

[4] Pitarke JM, Silkin VM, Chulkov EV, Echenique PM. Theory of surface plasmons and surface-plasmon polaritons. Reports on progress in physics. 2006, 70(1), 1. doi: 10.1088/0034-4885/70/1/R01.

[5] Muchuweni E, Mombeshora ET, Martincigh BS, Nyamori VO. Recent applications of carbon nanotubes in organic solar cells. Frontiers in Chemistry. 2022, 9, 733552. doi: 10.3389/fchem.2021.733552.

[6] Habisreutinger SN, Blackburn JL. Carbon nanotubes in high-performance perovskite photovoltaics and other emerging optoelectronic applications. Journal of Applied Physics. 2021, 129(1), 010903. doi: 10.1063/5.0035864.

[7] Moore K, Wei W. Applications of carbon nanomaterials in perovskite solar cells for solar energy conversion. Nano Materials Science. 2021, 3(3), 276-290. doi: 10.1016/j.nanoms.2021.03.005.

[8] Tian F, Sumikura H, Kuramochi E, Takiguchi M, Ono M, Shinya A, Notomi M. All-optical dynamic modulation of spontaneous emission rate in hybrid optomechanical emitter-cavity systems. Optica. 2022, 9(3), 309-316. doi: 10.1364/OPTICA.444781.

[9] Burlak G, Medina-Ángel G. Structure of optical Cherenkov radiation in a three-dimensional compound medium with carbon nanotubes. Journal of the Optical Society of America B. 2019, 36(2), 187-193. doi: 10.1364/JOSAB.36.000187.

[10] Burlak G, Cuevas-Arteaga C, Medina-Ángel G, Martínez-Sánchez E, Calderón-Segura YY. Plasmon-polariton oscillations in three-dimensional disordered nanotubes excited by a moving charge. Journal of Applied Physics. 2019, 126(1), 013101. doi: 10.1063/1.5098019.

[11] Burlak G, Medina-Ángel G, Martínez-Sánchez E. Condensation of plasmon-polaritons in dispersive carbon nanotubes assisted by a fast charge. Physica Scripta. 2021, 96(12), 125515. doi: 10.1088/1402-4896/ac2b46.

[12] Yanagi K, Okada R, Ichinose Y, Yomogida Y, Katsutani F, Gao W, Kono J. Intersubband plasmons in the quantum limit in gated and aligned carbon nanotubes. Nature communications. 2018, 9(1), 1121. doi: 10.1038/s41467-018-03381-y.
[13] Singh MR, Schindel DG, Hatef A. Dipole-dipole interaction in a quantum dot and metallic nanorod hybrid system. Applied Physics Letters. 2011, 99(18), 181106. doi: 10.1063/1.3658395.
[14] Terzis AF, Kosionis SG, Boviatsis J, Paspalakis E. Nonlinear optical susceptibilities of semiconductor quantum dot–metal nanoparticle hybrids. Journal of Modern Optics. 2016, 63(5), 451-461. doi: 10.1080/09500340.2015.1079655.
[15] Singh MR, Davieau K, Carson JJ. Effect of quantum interference on absorption of light in metamaterial hybrids. Journal of Physics D: Applied Physics. 2016, 49(44), 445103. doi: 10.1088/0022-3727/49/44/445103.
[16] Yannopapas, V., Paspalakis, E. Optical properties of hybrid spherical nanoclusters containing quantum emitters and metallic nanoparticles. Physical Review B. 2018, 97(20), 205433. doi: 10.1103/PhysRevB.97.205433.
[17] Singh MR. Theory of all-optical switching based on the Kerr nonlinearity in metallic nanohybrids. Physical Review A. 2020, 102(1), 013708. doi: 10.1103/PhysRevA.102.013708.
[18] Guo J, Black K, Hu J, Singh M. Study of plasmonics in hybrids made from a quantum emitter and double metallic nanoshell dimer. Journal of Physics. 2018, 30(18), 185301. doi: 10.1088/1361-648X/aab72b.
[19] Jackson JD. Classical Electrodynamics. New York, EU: John Wiley and Sons, 1998.
[20] Longe P, Bose SM. Collective excitations in metallic graphene tubules. Physical Review B. 1993, 48(24), 18239. doi: 10.1103/PhysRevB.48.18239.
[21] Yannouleas C, Bogachek EN, Landman U. Collective excitations of multishell carbon microstructures: Multishell fullerenes and coaxial nanotubes. Physical Review B. 1996, 53(15), 10225. doi: 10.1103/PhysRevB.53.10225.
[22] Wei L, Wang YN. Electromagnetic wave propagation in single-wall carbon nanotubes. Physics Letters A. 2004, 333(3-4), 303-309. 10.1103/PhysRevB.53.10225.
[23] Moradi A, Khosravi H. Plasmon dispersion in metallic carbon nanotubes in the presence of low-frequency electromagnetic radiation. Physics Letters A. 2007, 371(1-2), 1-6. doi: 10.1016/j.physleta.2007.05.110.
[24] Siegman AE. Laseres. Sausalito, California, EU: University Science Books, 1986.
[25] Taflove A, Hagness, SC, Piket-May, M. Computational electromagnetics: the finite-difference time-domain method. The Electrical Engineering Handbook. 2005, 3(629-670), 15. doi: 10.1016/B978-012170960-0/50046-3.
[26] Cao H, Zhao YG, Ho ST, Seelig EW, Wang QH, Chang RPH. Random laser action in semiconductor powder. Physical Review Letters. 1999, 82(11), 2278. doi: 10.1103/PhysRevLett.82.2278.
[27] Abramowitz M, Stegun IA. Handbook of Mathematical Functions: with Formulas, Graphs, and Mathematical Tables. New York, EU: Dover Books on Mathematics, 1965.
[28] Alexandrov AF, Bogdankevich LS, Rukhadze AA. Principles of plasma electrodynamics 9th ed. Berlin, Germany: Springer, 1984.

ABOUT THE AUTHORS

Dr. Gennadiy Burlak, estudió en la Universidad Nacional de Kiev (KNU), Ucrania, en el Departamento de Física Teórica. El Doctor en Ciencias Físico-Matemáticas. Trabajó como catedrático del Departamento de Física Teórica de KNU.
A partir de 1998 – a la fecha: Profesor Investigador Titular "C" del Centro de Investigación en Ingeniería y Ciencias Aplicadas de la Universidad Autónoma del Estado de Morelos, México, tiene SNI nivel 3. El Dr. Burlak es Merito estatal en categoría Investigación científica 2022.
El Dr. Burlak es autor y coautor de 12 libros y capítulos de libros, 175 artículos publicados en revistas internacionales, 186 ponencias en Congresos nacionales e internacionales. Bajo de su dirección han graduado: Doctorado: 8, de cuales 6 son miembros de SNI.
Líneas principales de investigación son: la percolación óptica, teoría electromagnética, microesferas multicapas, radiación óptica de nano-estructuras, entrelazamiento cuántico, física no-lineal, inteligencia artificial.

El Dr. Gustavo Medina Ángel, En 2008 estudio la Ingeniería en Sistemas Computacionales, egresado de Instituto Tecnológico de Zacatepec, en el 2016 se tituló como Maestro en Ingeniería y Ciencias Aplicadas de la Universidad Autónoma del Estado de Morelos y en el año 2020 obtuvo el título de Doctor en Ingeniería y Ciencias Aplicadas en la misma institución, actualmente es docente de la Facultad de Contaduría, Administración e Informática, así como en la escuela de Estudios Superiores de Mazatepec. Es desarrollador de Software Independiente, ha impartido talleres de programación avanzada en Java, programación en Arduino, Internet de las Cosas (IoT) y programación móvil. Ha publicado artículos nacionales e internacionales y se ha desempeñado como árbitro en revistas científicas. Las líneas de investigación a las que se dedica son; la simulación de fenómenos físicos, los métodos numéricos aplicados a la computación, la optimización de procesos y el procesamiento digital de imágenes.